

Properties of ρ and ω Mesons at Finite Temperature and Density as Inferred from Experiment

V. L. Eletsky^{1,2}, M. Belkacem^{1,3}, P. J. Ellis¹ and J. I. Kapusta¹

¹*School of Physics and Astronomy, University of Minnesota
Minneapolis, MN 55455, USA*

²*Institute for Theoretical and Experimental Physics
B. Cheremushkinskaya 25, Moscow 117218, Russia*

³*Laboratoire de Physique Quantique, Université Paul Sabatier
31062 Toulouse Cedex, France*

(October 24, 2018)

Abstract

The mass shift, width broadening, and spectral density for the ρ and ω mesons in a heat bath of nucleons and pions are calculated using a general formula which relates the self-energy to the real and imaginary parts of the forward scattering amplitude. We use experimental data to saturate the scattering amplitude at low energies with resonances and include a background Pomeron term, while at high energies a Regge parameterization is used. The real part obtained directly is compared with the result of a dispersion integral over the imaginary part. The peaks of the spectral densities are little shifted from their vacuum positions, but the widths are considerably increased due to collisional broadening. Where possible we compare with the UrQMD model and find quite good agreement. At normal nuclear matter density and a temperature of 150 MeV the spectral density of the ρ meson has a width of 345 MeV, while that for the ω is in the range 90–150 MeV.

11.10.Wx, 25.75.-q, 12.40.Vv

I. INTRODUCTION

The modification of the free space properties of a vector meson in hadronic or nuclear matter is an important problem which has attracted much attention. Among the properties of immediate interest are the mass shift and width broadening of the particle in a medium. Many authors have studied these questions for the ρ meson, and also in some cases the ω meson, at zero temperature in equilibrium nuclear matter, see the reviews of Ref. [1] and Refs. [2–6]. More closely related to this paper is the finite temperature work of Rapp *et al.* [7,8] who have considered the medium modification of the pions comprising the meson, as well as additional medium scattering contributions. There have also been studies [9,10] of ω and ρ mesons in a pion heat bath, although we shall see that nucleons produce a larger effect. QCD sum rules have also been employed [1,3], but these are tailored to the small distance behavior whereas, as Eletsky and Ioffe [2] have pointed out, the self-energy is determined by meson-nucleon scattering at relatively large distances of order 1 fm; see also Ref. [11].

Many of these works have relied on effective Lagrangians; however, we would like to adopt as model-independent an approach as possible. Therefore we use experimental data to construct the amplitude for vector mesons scattering from pions and nucleons. The low energy region is described in terms of resonances plus background, while at high energies a Regge model is employed. In principle the amplitude should be completely determined by the data. In practice there are uncertainties because the data are often inaccurate and incomplete, particularly for the ω meson. It is therefore important to check that the real and imaginary parts of our amplitudes approximately satisfy the dispersion relation which follows from the analytic properties of the amplitude. Using our amplitude the in-medium self-energy of the ρ and ω mesons can be calculated at finite temperature and density. We use the leading term of the exact self-energy expansion [12] which requires that the densities be sufficiently small that only single scatterings are important. Where possible we will compare with results from the ultra-relativistic quantum molecular dynamics (UrQMD) model [13] which has been extensively tested. For the ρ meson this paper represents an updated and improved version of earlier work [14] hereinafter referred to as EIK.

This paper is organized as follows. In Sec. II we discuss the formalism, parameters and results for the scattering amplitudes. These are employed in Sec. III where the self-energies of the ρ and ω mesons are presented. Concluding remarks are given in Sec. IV.

II. SCATTERING AMPLITUDES

A. Low Energy Amplitude

We assume that the self-energies of the isovector ρ and isoscalar ω vector mesons are dominated by scattering from the pions and nucleons present in a heat bath. Accordingly we need four scattering amplitudes. We will adopt the two-component duality approach due to Harari [15] (see also Collins [16]) which states that while ordinary Reggeons are dual to

s -channel resonances, the Pomeron is dual to the background upon which the resonances are superimposed. Taking for definiteness the case of a ρ meson scattering from particle a , we write the forward scattering amplitude in the c.m. system as

$$f_{\rho a}^{\text{cm}}(s) = \frac{1}{2q_{\text{cm}}} \sum_R W_{\rho a}^R \frac{\Gamma_{R \rightarrow \rho a}}{M_R - \sqrt{s} - \frac{1}{2}i\Gamma_R} - \frac{q_{\text{cm}} r_P^{\rho a} (1 + \exp^{-i\pi\alpha_P})}{4\pi s \sin \pi\alpha_P} s^{\alpha_P}. \quad (1)$$

Here the first term involves a sum over a series of Breit-Wigner resonances of mass M_R and total width Γ_R , while the second term is the Pomeron background contribution which is discussed in Sec. II B below. No background contribution was included in EIK [14]. For the Breit-Wigner term we have used the non-relativistic form which amounts to setting $M_R + \sqrt{s} \simeq 2M_R$ in the relativistic denominator $M_R^2 - s - i\Gamma_R M_R$. This has a negligible effect on the results we present. In the usual notation \sqrt{s} is the total c.m. energy and the magnitude of the c.m. momentum is

$$q_{\text{cm}} = \frac{1}{2} \sqrt{[s - (m_\rho + m_a)^2][s - (m_\rho - m_a)^2]} / \sqrt{s}. \quad (2)$$

The statistical averaging factor for spin and isospin is

$$W_{\rho a}^R = \frac{(2s_R + 1)}{(2s_\rho + 1)(2s_a + 1)} \frac{(2t_R + 1)}{(2t_\rho + 1)(2t_a + 1)}, \quad (3)$$

in an obvious notation. Since we are averaging over all spin directions we shall not distinguish longitudinal and transverse polarizations. The isospin averaging implies that all charge states of particle a are equally populated so there is no medium-induced mixing [17] between the ρ and ω mesons. In eq. (1) $\Gamma_{R \rightarrow \rho a}$ represents the partial width for the resonance decay into the ρa channel. If we denote the c.m. momentum at resonance by q_{cm}^R , then for $q_{\text{cm}} \geq q_{\text{cm}}^R$ we use the value obtained from the total width and the branching ratio on resonance. However the threshold behavior of the partial width is known and we incorporate this for $q_{\text{cm}} \leq q_{\text{cm}}^R$ by replacing $\Gamma_{R \rightarrow \rho a}$ by $\Gamma_{R \rightarrow \rho a} (q_{\text{cm}}/q_{\text{cm}}^R)^{2l+1}$, where l is the relative angular momentum between the ρ and the a . Since the total width is the sum of the partial widths this dependence should be incorporated in Γ_R . We do this in the case that a is a pion, but when a is a nucleon there are many decay channels and it becomes impractical, so we simply take Γ_R to be a constant.

For the case of ρN scattering we use the N^* and Δ^* resonances from Manley and Saleski [18] which are listed in Table I. These provide a better match onto the high energy region than the fit of Vrana *et al.* [19]. It is also necessary to include the $\Delta(1232)$ and the $N(1520)$ subthreshold resonances since they make a substantial contribution. In order to estimate the widths we assume that the vector dominance model is valid, even though it is better suited to high energies. This allows us to relate the photon and ρ widths. Specifically, since both resonances are close to the ρN threshold, we can write for each of them $\Gamma_{\rho N} = q_{\text{cm}} \gamma_{\rho N}$ and $\Gamma_{\gamma N} = k_{\text{cm}} \gamma_{\gamma N}$, where k_{cm} is γN c.m. momentum. Then vector dominance gives

$$\gamma_{\gamma N} = 4\pi\alpha \frac{1}{g_\rho^2} \left(1 + \frac{g_\rho^2}{g_\omega^2} \right) \gamma_{\rho N}, \quad (4)$$

where α is the fine structure constant. For the coupling to the photon we take $g_\rho^2/4\pi = 2.54$ and $g_\rho^2/g_\omega^2 = 1/8$. The value of $\gamma_{\gamma N}$ can be deduced from the decay width and the photon branching ratio of the resonances [20].

For the case of ωN much less information is available, although better data is expected in the future [21]. Therefore we adopt two extreme models with the expectation that reality lies somewhere between the two. The first we refer to as the two resonance model since, in addition to the subthreshold $N(1520)$, we include the two resonances reported by Manley and Saleski [18]. These are the $N(1900)$ [$\Gamma_R = 498$ MeV, branching ratio to ωN 0.30] and the $N(2190)$ [$\Gamma_R = 547$ MeV, branching ratio 0.49]. It must be stressed that there is uncertainty in these assignments; for example, Vrana *et al.* [19] report ωN strength only for the $N(2190)$ with a roughly similar width and branching ratio. For the second model, motivated by the fact that the ρ and ω differ only in isospin, we use for the ω the same $T = \frac{1}{2}$ N^* resonances as for the ρ with the same partial widths, except that we omit the $N(1720)$ since it decays 75–80% in the ρN channel [20]. In the other cases the errors are sufficiently large that similar ρ and ω decays could be accommodated. We refer to this as the multi-resonance model. We also examined the alternative procedure of adopting the decay widths in the ωN channel for the resonances found in the quark model calculations of Capstick and Roberts [22]. We found, however, that the cross section was too small for satisfactory matching onto the high energy part.

Turning now to the $\rho\pi$ amplitude, Eq. (1) indicates that a Breit-Wigner contribution for s -waves in the limit $q_{\text{cm}} \rightarrow 0$ is a constant since a factor of q_{cm} is included in the partial width. According to Adler's theorem the pion scattering amplitude on any hadronic target vanishes when $q_{\text{cm}} \rightarrow 0$ in the limit of massless pions. In the framework of an effective Lagrangian this can be achieved if a derivative coupling is used for the pion field, $\partial_\mu \pi$. We assume that the term in the Lagrangian responsible for $\rho\pi \rightarrow a_1(1260)$ involves $\partial_\mu \pi$ multiplied by the ρ -meson field strength tensor $\rho^{\mu\nu}$ and \mathbf{a}_ν for the a_1 field. This gives an additional factor which should be included for an s -wave partial width of

$$\left(\frac{s - m_\rho^2 - m_\pi^2}{s_0 - m_\rho^2 - m_\pi^2} \right)^2, \quad (5)$$

for $s \leq s_0$, where s_0 is a normalization point. When $s \geq s_0$ this factor is replaced by unity. Since this is a soft pion effect it is reasonable to cut it off when $q_{\text{cm}} \sim 1 - 2m_\pi$, hence we take the normalization point to be $s_0 = (m_\rho + 2m_\pi)^2$. We believe this is more reasonable than taking the resonance mass for $\sqrt{s_0}$ as in EIK [14]. The analogous factor is also introduced for the $h_1(1170)$ resonance. The parameters [20] for these and the other meson resonances included in the calculation are listed in Table I. For the $\omega\pi$ amplitude only the $b_1(1235)$ is listed as having appreciable strength [20]. We take it to decay 100% to $\omega\pi$ with a width of 142 MeV and apply the Adler factor as outlined above.

B. High Energy Amplitude

The high energy forward scattering amplitude is known [23] to be well approximated by the Regge form

$$f_{\rho a}^{\text{cm}}(s) = -\frac{q_{\text{cm}}}{4\pi s} \sum_i \frac{1 + \exp^{-i\pi\alpha_i}}{\sin \pi\alpha_i} r_i^{\rho a} s^{\alpha_i}. \quad (6)$$

We shall consider a Pomeron term P and a Regge term P' . In order to obtain the intercept α_i and the residue r_i for the i 'th Regge pole trajectory we use the relation between the amplitude and the total cross section given by the optical theorem: $\sigma_{\rho a} = 4\pi \text{Im} f_{\rho a}^{\text{cm}}/q_{\text{cm}}$. High energy scattering is dominated by contributions from individual quarks – the additive quark model. Therefore it is reasonable to average over charge states and take the cross section $\sigma_{\rho N} \simeq \sigma_{\pi N}$. Using the Particle Data Group listing [20] this gives intercepts $\alpha_P = 1.093$ and $\alpha_{P'} = 0.642$ with $r_P^{\rho N} = 11.88$ and $r_{P'}^{\rho N} = 28.59$ (the units yield a cross section in mb with energies in GeV). We would like to take $\sigma_{\rho\pi} \simeq \sigma_{\pi\pi}$, averaged over charge states. Of course data for the latter are not available, but for Regge exchange in the t -channel it is appropriate to invoke factorization [24] so that the residue $r_P^{\rho\pi} \simeq r_{P'}^{\pi\pi} \simeq (r_P^{\pi N})^2/r_P^{NN} = 7.508$, using Ref. [20]. Similarly $r_{P'}^{\rho\pi} = 12.74$. The intercepts α_i are universal. These parameters yield cross sections which are roughly 30% smaller than in EIK [14] where the γN and $\gamma\pi$ cross sections were employed along with vector dominance. This, together with the background term in Eq. (1), allows us to satisfy the dispersion relation (see below) significantly more accurately than with the EIK parameterization [14].

Since the different isospin structure of the ρ and the ω is expected to be insignificant at high energy, we adopt the same parameterization for the $\omega\pi$ and ωN scattering amplitudes as for the $\rho\pi$ and ρN amplitudes. The parameters for the Pomeron obtained here are also used for the background term in Eq. (1). Note that if the Pomeron intercept α_P were exactly 1, the Pomeron amplitude would be pure imaginary.

C. Results

Since we shall work in the rest frame of the heat bath we will give the scattering amplitude for the case that particle a is at rest. This is related to the c.m. amplitude by

$$f_{\rho a}(E_\rho) = \frac{\sqrt{s}}{m_a} f_{\rho a}^{\text{cm}}(s), \quad (7)$$

where

$$E_\rho - m_\rho = \frac{s - (m_\rho + m_a)^2}{2m_a}. \quad (8)$$

The imaginary parts of $f_{\rho a}$ and $f_{\omega a}$ are shown in Fig. 1. In most cases the low energy part contains a number of overlapping resonances so that the structure is washed out. The

exception is the case of the $\omega\pi$ amplitude where the single b_1 resonance is clearly visible (note that this amplitude is the same in the middle and lower panels). Because of the kinematics, Eq. (8), the resonance region ends at $E_\rho - m_\rho \sim 1$ GeV for ρN and ~ 4 GeV for $\rho\pi$ and it is matched onto the Regge part slightly beyond these points. At low energies the ρN amplitude is of similar magnitude to the ωN amplitude in the multi-resonance model, but it is much smaller in the two-resonance model. This is less marked for the real part of the amplitude, given in Fig. 2, where the two ωN amplitudes are more similar and both are smaller in magnitude than the ρN amplitude in this resonance region. The pion scattering amplitudes display the change in sign expected for Breit-Wigner resonances. This is not seen in the nucleon case because of the subthreshold resonances included here. These are neglected by Kondratyuk *et al.* [4] which may be the reason that their ρN amplitude becomes slightly positive at small momenta; it is also somewhat larger in magnitude at large momenta. They obtained their result from a dispersion integral over an imaginary amplitude constructed from resonances at low energy and vector dominance together with photon cross sections at high energy.

The scattering amplitude should obey a once-subtracted dispersion relation relating the real part to a principal value integral over the imaginary part:

$$\text{Re}f_{\rho a}(E_\rho) = \text{Re}f_{\rho a}(0) + \frac{2E_\rho^2}{\pi} \text{P.V.} \int_{m_\rho}^{\infty} \frac{\text{Im}f_{\rho a}(E')dE'}{E'(E'^2 - E_\rho^2)}. \quad (9)$$

Thus one can compare the analytical real part of Secs. II A and B with the result from Eq. (9); the difference should be the constant $\text{Re}f_{\rho a}(0)$. This does not hold if one uses the Regge form for f at all energies, the difference only becomes exactly constant if the lower limit of the integration is arbitrarily taken to be the point where $s = 0$ [16]. Alternatively, if one assumes a pure resonance form for the amplitude the aforementioned difference is not constant either. In both cases noticeable deviations from constancy start to appear at energies $E_\rho - m_\rho$ below about 2 GeV. This trend is also seen for the differences when the actual amplitudes are used, as displayed in Fig. 3. The nucleon amplitudes give the most reasonable account of the dispersion relation, with the ωN two-resonance case showing a larger deviation from constancy than the other two cases. For pion scattering the deviations are larger, although it should be borne in mind that the amplitudes themselves are larger too. Of course one would not expect phenomenological approximations to precisely obey the stringent constraints which follow from the analytic properties of the amplitude, and in that light we view the results in Fig. 3 as reasonable. We remark that we have considered variations in the parameters involved in the amplitude and have not obtained improvement. In particular, omission of the background Pomeron term in Eq. (1) gives much worse results.

There are inevitable uncertainties in a phenomenological parameterization of a scattering amplitude so it is useful to compare with other work. Here we contrast total cross sections calculated from the imaginary parts of the amplitudes discussed above with those used in the UrQMD model [13]. The latter employs a resonance description at the lower

energies without, however, a background term. At the higher energies the CERN–HERA parameterizations [20] are used, together with the additive quark model, leading to color string excitations. Comparison of the cross sections for scattering from pions in Fig. 4 shows quite close agreement except at the lowest energies. Here the UrQMD cross sections increase because no factor of $(q_{\text{cm}}/q_{\text{cm}}^R)^{2l+1}$ is included in the width, nor is the Adler factor included. Since physically the cross section should go to zero in the chiral limit of massless pions we prefer our result where the cross sections are small. Note that precisely at threshold, $\sqrt{s} = m_\rho + m_\pi$, both approaches give a divergent cross section which, however, is of no consequence for the calculation of the self energies. The corresponding results for the nucleon cross sections are given in Fig. 5. Again there is very close agreement at high energies, but less good agreement at low energies. For the ρ the basic difference is that UrQMD joins the string region to the resonance region at a lower energy. In fact our cross section compares better with that of Kondratyuk *et al.* [4]. For the ω cross section only the $N(1900)$ resonance is included in the UrQMD model, whereas we also include the $N(2190)$. This can be seen rather clearly in the lower panel for the two-resonance model. Naturally our multi-resonance model for the ω bears little resemblance to UrQMD (middle panel) at low energies, being closer to the ρN case. Apart from this we would say that there is broad agreement between UrQMD and the present results.

III. SELF-ENERGIES OF THE VECTOR MESONS

For a ρ meson scattering from hadron a in the medium the contribution to the retarded self-energy [12,14] is:

$$\Pi_{\rho a}(E, p) = -4\pi \int \frac{d^3k}{(2\pi)^3} n_a(\omega) \frac{\sqrt{s}}{\omega} f_{\rho a}^{\text{cm}}(s), \quad (10)$$

where E and p are the energy and momentum of the ρ meson, $\omega^2 = m_a^2 + k^2$, and n_a is either a Bose-Einstein or Fermi-Dirac occupation number as appropriate for particle a . If the self-energy is evaluated on shell in the rest frame of a it is possible to do all the angular integrations, giving

$$\Pi_{\rho a}(p) = -\frac{m_\rho m_a T}{\pi p} \int_{m_a}^{\infty} d\omega \ln \left[\frac{1 - \exp(-\omega_+/T)}{1 - \exp(-\omega_-/T)} \right] f_{\rho a} \left(\frac{m_\rho \omega}{m_a} \right), \quad (11)$$

where $\omega_\pm = (E\omega \pm pk)/m_\rho$ and a is a boson. If a is a fermion ω_\pm has an additional chemical potential contribution $-\mu$ and the argument of the logarithm becomes $[1 + \exp(-\omega_-/T)]/[1 + \exp(-\omega_+/T)]$.

The total self-energy is given by summing over all target species and including the vacuum contribution

$$\Pi_\rho^{\text{tot}}(E, p) = \Pi_\rho^{\text{vac}}(M) + \Pi_{\rho\pi}(p) + \Pi_{\rho N}(p). \quad (12)$$

Here the vacuum part of Π can only depend on the invariant mass, $M = \sqrt{E^2 - p^2}$, whereas the matter parts can in principle depend on E and p separately. However, in the approximation we are using the scattering amplitudes are of necessity evaluated on the mass shell of the ρ meson. This means that the matter parts only depend on p because M is fixed at m_ρ . The dispersion relation is determined from the poles of the propagator with the self-energy evaluated on shell, *i.e.* $M = m_\rho$. Taking again for definiteness the case of the ρ we have

$$E^2 = m_\rho^2 + p^2 + \Pi_\rho^{\text{tot}}(p) . \quad (13)$$

Since the self-energy has real and imaginary parts so does $E(p) = E_R(p) - i\Gamma(p)/2$. The width is given by

$$\Gamma(p) = -\text{Im}\Pi_\rho^{\text{tot}}(p)/E_R(p) , \quad (14)$$

with

$$2E_R^2(p) = p^2 + m_\rho^2 + \text{Re}\Pi_\rho^{\text{tot}}(p) + \sqrt{[p^2 + m_\rho^2 + \text{Re}\Pi_\rho^{\text{tot}}(p)]^2 + [\text{Im}\Pi_\rho^{\text{tot}}(p)]^2} . \quad (15)$$

The width of the ρ -meson in vacuum, $\Gamma_\rho^{\text{vac}} = -\text{Im}\Pi_\rho^{\text{vac}}/m_\rho$, is 150 MeV (the width of the ω -meson in vacuum is 8.4 MeV). We define the mass shift to be

$$\Delta m_\rho(p) = \sqrt{m_\rho^2 + \text{Re}\Pi_\rho^{\text{tot}}(p)} - m_\rho . \quad (16)$$

We assume that the hadronic matter can be considered to be a weakly interacting gas of pions and nucleons. In order to test this assumption we have run the UrQMD code in a box for baryon densities up to twice normal nuclear matter density at temperatures up to 150 MeV. The results show that more than 95% of all ρ -meson scatterings occur from pions and nucleons so that it is reasonable to focus on these interactions. We will consider nucleon densities of $n_N = 0, 1$ and 2 in units of equilibrium nuclear matter density ($n_0 = 0.16$ nucleons/fm³). We assume that the system is in thermal equilibrium with a temperature below 170 MeV so that hadrons are the appropriate degrees of freedom rather than quarks and gluons. For densities of 1 and 2 the nucleon chemical potentials are, respectively, 747 and 821 MeV at $T = 100$ MeV, and 543 and 650 MeV at $T = 150$ MeV. Anti-nucleons are not included.

The vector meson widths are shown as a function of momentum in Fig. 6 for two temperatures and three nucleon densities. Note that the widths given here are defined to be in the rest frame of the thermal system. (The present results replace those of Eletsky and Kapusta [14] since the weighting of the pion contribution was too small there due to a computer code error. The nucleon contributions still dominate, however.) For Γ_ρ the $n_N = 0$ results are little changed from the vacuum value until temperatures of the order of the pion mass are reached. At $T = 150$ MeV the width generated by collisions with pions is about 50 MeV. This is a factor of two larger than obtained by Haglin [9] using an effective Lagrangian, but a little less than the 80 MeV reported by Rapp and Gale [7]. Interactions

with nucleons give a 100 MeV contribution to the width at $n_N = 1$, similar to the zero temperature estimate of Kondratyuk *et al.* [4], and about twice that at $n_N = 2$. Thus at the highest temperatures and densities the width is 2–3 times the vacuum value and is becoming comparable to the mass. The middle and lower panels of Fig. 6 are the same for $n_N = 0$ since nucleons are not involved in this case. Here the effect of increasing the temperature, and therefore the pion density, is much more marked than for the ρ since the vacuum width of the ω is so small. At $T = 150$ MeV the width is about 50 MeV which is similar to the value obtained by Schneider and Weise [10] in an effective Lagrangian approach, but a factor of two larger than given by Haglin [9]. When the nucleon density is non-zero we expect nature to lie somewhere between the larger widths given by the multi-resonance model (middle panel) and the smaller widths given by the two-resonance model (lower panel). The functional dependence on p differs in the two cases. However, for a temperature of 150 MeV and $n_N = 1$, Γ_ω is expected to lie between 100 and 150 MeV. This is an enhancement of the vacuum width by a factor of 12–18, which is in line with Rapp’s estimate [8] of a factor of 20 at a slightly higher temperature of 180 MeV.

In the UrQMD model collisional widths can be obtained by allowing a volume of matter to come to equilibrium at a given temperature and baryon density [25]. Then the average time between collisions of a ρ meson with a given species, N or π , can be determined. The reciprocal of this gives the width due to collisional broadening (in units with $\hbar = 1$). In order for the notion of thermodynamic equilibrium to make sense detailed balance must hold. Therefore, for present purposes, it is necessary to drop the string contribution and retain only the resonance contribution [25]. Thus the results should be most reliable at low momenta. We show the UrQMD results for the collisional broadening due to scattering from pions and nucleons separately in Fig. 7. They are compared with the results discussed above for two representative cases of baryon density, n_B , and temperature. For $n_B = \frac{1}{2}$ with $T = 100$ MeV and $n_B = 2$ with $T = 150$ MeV, the baryon chemical potentials are 630 and 479 MeV, respectively, which correspond to nucleon densities $n_N \simeq \frac{1}{3}$ and $n_N \simeq \frac{2}{3}$, with all densities in units of n_0 . The present results agree quite nicely with UrQMD at low momenta, suggesting that interference between sequential scatterings can be ignored at these temperatures and densities as we have done. The deviations at larger momenta give some measure of the role played by the high energy Regge part of the scattering amplitude.

The mass shifts for the vector mesons are displayed in Fig. 8. They turn out to be quite small, at most a few tens of MeV. For both the ρ and the ω mesons the interaction with pions alone ($n_N = 0$) produces a small negative Δm , while the introduction of nucleons gives a positive contribution. For the two ω models at zero momentum Δm_ω is in the range -15 to $+15$ MeV. On the other hand at $p = 1500$ MeV for $n_N = 2$, Δm_ω is 30 MeV in the two-resonance model and 50 MeV in the multi-resonance model, somewhat smaller than $\Delta m_\rho = 60$ MeV. These trends and numbers for the vector meson mass shifts are roughly consistent with other analyses [5,7,8,10]. However, in nuclear matter at zero temperature the coupled-channel calculation of Friman *et al.* [6] gives larger shifts and, for the ω , so does the chiral approach of Klingl *et al.* [3].

The rate of dilepton production is directly proportional to the imaginary part of the photon self-energy [26,27] which is itself proportional to the imaginary part of the ρ meson propagator because of vector meson dominance [28,29].

$$E_+ E_- \frac{dR}{d^3p_+ d^3p_-} \propto \frac{-\text{Im}\Pi_\rho^{\text{tot}}}{[M^2 - m_\rho^2 - \text{Re}\Pi_\rho^{\text{tot}}]^2 + [\text{Im}\Pi_\rho^{\text{tot}}]^2}, \quad (17)$$

where, as before, M is the invariant mass. For the ρ -meson the vacuum part Π_ρ^{vac} can be obtained from the Gounaris-Sakurai formula [28,29]. This formula gives a very good description of the pion electromagnetic form factor, as measured in e^+e^- annihilation [30], up to 1 GeV apart from a small mixing with the ω meson which we are ignoring in this paper.

$$\begin{aligned} \text{Re}\Pi_\rho^{\text{vac}} = & \frac{g_\rho^2 M^2}{48\pi^2} \left[\left(1 - 4m_\pi^2/M^2\right)^{3/2} \ln \left| \frac{1 + \sqrt{1 - 4m_\pi^2/M^2}}{1 - \sqrt{1 - 4m_\pi^2/M^2}} \right| + 8m_\pi^2 \left(\frac{1}{M^2} - \frac{1}{m_\rho^2} \right) \right. \\ & \left. - 2 \left(\frac{p_0}{\omega_0} \right)^3 \ln \left(\frac{\omega_0 + p_0}{m_\pi} \right) \right], \end{aligned} \quad (18)$$

$$\text{Im}\Pi_\rho^{\text{vac}} = -\frac{g_\rho^2 M^2}{48\pi} \left(1 - 4m_\pi^2/M^2\right)^{3/2}. \quad (19)$$

Here $2\omega_0 = m_\rho = 2\sqrt{m_\pi^2 + p_0^2}$. The vacuum width is $\Gamma_\rho^{\text{vac}} = (g_\rho^2/48\pi)m_\rho(p_0/\omega_0)^3$ and the real part vanishes on shell. Since the vacuum decay of the ω into three pions is more complicated, while the width is tiny, we simply treat it as a constant except for the application of a non-relativistic phase space factor $[(M^2 - 9m_\pi^2)/(m_\omega^2 - 9m_\pi^2)]^2$ from threshold to $M = m_\omega$. A possible real vacuum contribution is ignored.

The imaginary part of the propagator, proportional to the spectral density, is plotted as a function of M in Fig. 9 for a temperature of 150 MeV. Pions alone have a small effect on the spectral density so we display results at $n_N = \frac{1}{2}, 1$ and 2. These parameters are characteristic of the final stages of a high energy heavy ion collision. As seen from Fig. 9 there is little change in the position of the peak, but the spectral density is greatly broadened. (In nuclear matter at $T = 0$ Refs. [5,6] obtain a more complicated structure.) Figure 9 shows that for $n_N = 1$ the width of the ρ peak (full width, half maximum) is 345 MeV which is becoming comparable to the mass of ρ meson and is consistent with the results of Rapp [8]. For the ω meson at this density the peak width is 150 MeV in the multi-resonance model and 90 MeV for the two-resonance model, while Rapp's width is intermediate between these values.

IV. CONCLUSIONS

In this paper we have described the scattering amplitudes for ρ and ω -mesons in terms of resonances plus background at low energies matched onto a Regge form at high energies

(our amplitudes are available upon request). The parameters were taken from experimental data in order to be as model independent as possible. Of course the data are imperfect, particularly for the ω meson where we adopted two extreme models with reality expected to lie somewhere between the two. Assuming that only single scatterings are important, as appears to be justified by comparison with the UrQMD results, it is then straightforward to obtain the self-energy at finite density and temperature.

Our results indicate for the shift in the pole mass a negative contribution from interactions with pions and a positive contribution from interactions with nucleons. The net result is small, at most a few tens of MeV. Thus the peak of the spectral density is little shifted, but the width is increased considerably due to collisions in the medium. Collisions with nucleons dominate, but the effect of pions is not negligible. At equilibrium nuclear matter density and a temperature of 150 MeV the width of the spectral density is 345 MeV for the ρ meson, about twice the vacuum width. For the ω meson the width is expected to lie between the values of 90 MeV and 150 MeV given by our two extreme models, a considerable change from the vacuum width of just 8.4 MeV. Where possible we have compared with the UrQMD model and found quite reasonable agreement. Our results are also quite consistent with those of Rapp and coworkers [7,8] and Schneider and Weise [10].

The next step is to use our results in a space-time model of the evolution of matter in high energy heavy ion collisions. This will allow us to study the extent to which our spectral densities are able to reproduce the observed e^+e^- mass spectra [31]. Such work is underway.

ACKNOWLEDGMENTS

We are indebted to B. L. Ioffe for valuable discussions. This work was supported in part by the US Department of Energy grant DE-FG02-87ER40382 and in part by the US Civilian Research & Development Foundation grant RP2-2247.

REFERENCES

- [1] C. Adami and G.E. Brown, Phys. Rep. **234**, 1 (1993); T.D. Cohen, R.J. Furnstahl, D.K. Griegel and X. Jin, Prog. Part. Nucl. Phys. **35**, 221 (1995); T.Hatsuda, H. Shiomi and H. Kuwabara, Prog. Theor. Phys. **95**, 1009 (1996).
- [2] V.L. Eletsky and B.L. Ioffe, Phys. Rev. Lett. **78**, 1010 (1997).
- [3] F. Klingl, N. Kaiser and W. Weise, Nucl. Phys. **A624**, 527 (1997).
- [4] L.A. Kondratyuk, A. Sibirtsev, W. Cassing, Ye.S. Golubeva and M. Effenberger, Phys. Rev. C **58**, 1078 (1998).
- [5] M. Post, S. Leupold and U. Mosel, nucl-th/0008027; M. Post and U. Mosel, nucl-th/0008040; U. Mosel and M. Post, nucl-th/0103059.
- [6] B. Friman, M. Lutz and G. Wolf, nucl-th/0003012, *Proceedings Hirschegg 2000, Hadrons in Dense matter* (GSI, Darmstadt, Germany, 2000), ed. M. Buballa, W. Nörenberg, B.-J. Schaeffer and J. Wambach, p. 61.
- [7] R. Rapp, G. Chanfray and J. Wambach, Nucl. Phys. **A617**, 472 (1997); Phys. Rev. C **57**, 916 (1998); R. Rapp and C. Gale, Phys. Rev. C **60**, 024903 (1999).
- [8] R. Rapp, hep-ph/0010101.
- [9] K. Haglin, Nucl. Phys. **A584**, 719 (1995).
- [10] R.A. Schneider and W. Weise, hep-ph/0102189.
- [11] S. Mallik and A. Nyffeler, hep-ph/0102062.
- [12] S. Jeon and P.J. Ellis, Phys. Rev. D **58**, 045013 (1998).
- [13] S.A. Bass, *et al.*, Prog. Part. and Nucl. Phys. **41**, 225 (1998).
- [14] V.L. Eletsky, B.L. Ioffe and J.I. Kapusta, Eur. J. Phys. A **3**, 381 (1998); V.L. Eletsky and J.I. Kapusta, Phys. Rev. C **59**, 2757 (1999).
- [15] H. Harari, Phys. Rev. Lett. **20**, 1395 (1968).
- [16] P.D.B. Collins, *An Introduction to Regge Theory and High Energy Physics* (Cambridge University Press, Cambridge, UK, 1977).
- [17] A.K. Dutt-Mazumder, B. Dutta-Roy and A. Kundu, Phys. Lett. **B399**, 196 (1997).
- [18] D.M. Manley and E.M. Saleski, Phys. Rev. D **45**, 4002 (1992).
- [19] T.P. Vrana, S.A. Dytman and T.-S.H. Lee, Phys. Rep. **328**, 181 (2000).
- [20] Particle Data Group: D.E. Groom *et al.*, Eur. Phys. J. C **15**, 1 (2000).
- [21] J.J. Manak, V. Burkert, F. Klein, B. Mecking, A. Coleman and H. Funsten, Nucl. Phys. **A663**, 671 (2000).
- [22] S. Capstick and W. Roberts, Phys. Rev. D **49**, 4570 (1994).
- [23] A. Donnachie and P.V. Landshoff, Phys. Lett. **B296**, 227 (1992).
- [24] R.C. Brower, R.N. Cahn and J. Ellis, Phys. Rev. D **7**, 2080 (1973); R.D. Field and G.C. Fox, Nucl. Phys. **B80**, 367 (1974); K.G. Boreskov, A.B. Kaĭdalov and L.A. Ponomarev, Sov. J. Nucl. Phys. **21**, 84 (1975).
- [25] M. Belkacem, *et al.*, Phys. Rev. C **58**, 1727 (1998).
- [26] L.D. McLerran and T. Toimela, Phys. Rev. D **31**, 545 (1985).
- [27] H.A. Weldon, Phys. Rev. D **42**, 2384 (1990).
- [28] G.J. Gounaris and J.J. Sakurai, Phys. Rev. Lett. **21**, 244 (1968).

- [29] C. Gale and J.I. Kapusta, Nucl. Phys. **B357**, 65 (1991).
- [30] R.F. Schwitters and K. Strauch, Annu. Rev. Nucl. Sci. **26**, 89 (1976).
- [31] B. Lenkeit *et al.* (CERES Collaboration), Nucl. Phys. **A661**, 23c (1999).

TABLES

TABLE I. Baryon and Meson Resonances Included in the ρ Amplitude

Resonance	Mass (GeV)	Width (GeV)	Branching ratio (ρN or $\rho\pi$)
$N(1700)$	1.737	0.249	0.13
$N(1720)$	1.717	0.383	0.87
$N(1900)$	1.879	0.498	0.44
$N(2000)$	1.903	0.494	0.60
$N(2080)$	1.804	0.447	0.26
$N(2090)$	1.928	0.414	0.49
$N(2100)$	1.885	0.113	0.27
$N(2190)$	2.127	0.547	0.29
$\Delta(1700)$	1.762	0.599	0.08
$\Delta(1900)$	1.920	0.263	0.38
$\Delta(1905)$	1.881	0.327	0.86
$\Delta(1940)$	2.057	0.460	0.35
$\Delta(2000)$	1.752	0.251	0.22
$\phi(1020)$	1.020	0.0045	0.13
$h_1(1170)$	1.170	0.36	1
$a_1(1260)$	1.230	0.40	0.68
$\pi(1300)$	1.300	0.40	0.32
$a_2(1320)$	1.318	0.107	0.70
$\omega(1420)$	1.419	0.174	1

FIGURES

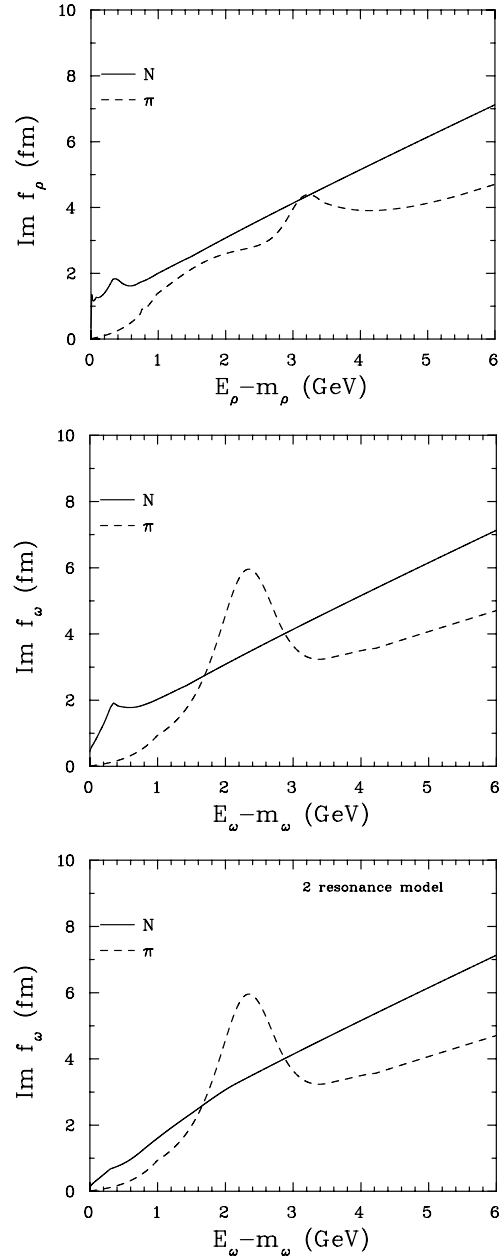


FIG. 1. The imaginary part of the amplitude for ρa and ωa scattering with $a = N, \pi$. For the ω meson we show results for the multi-resonance model and the two-resonance model.

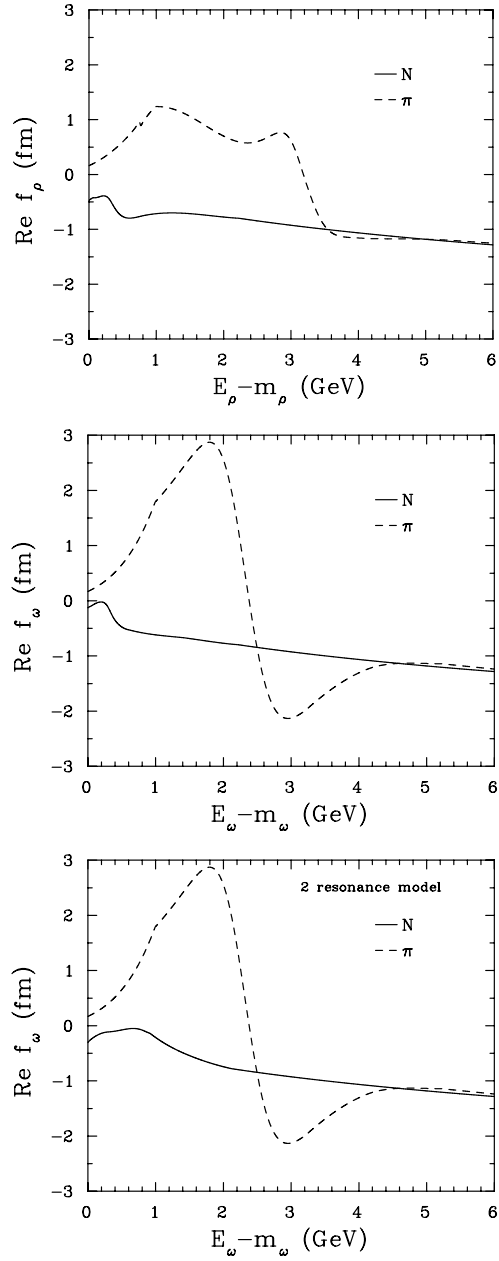


FIG. 2. As for Fig. 1, but the real parts of the amplitudes.

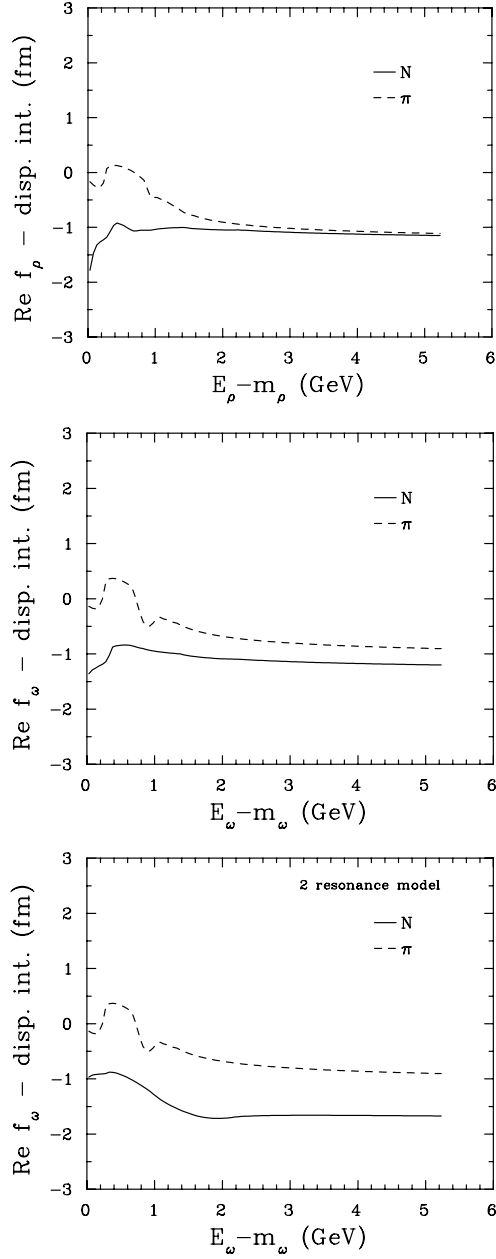


FIG. 3. Difference between the real part of the amplitudes given in Fig. 2 and those deduced from the imaginary parts of Fig. 1 via the dispersion relation.

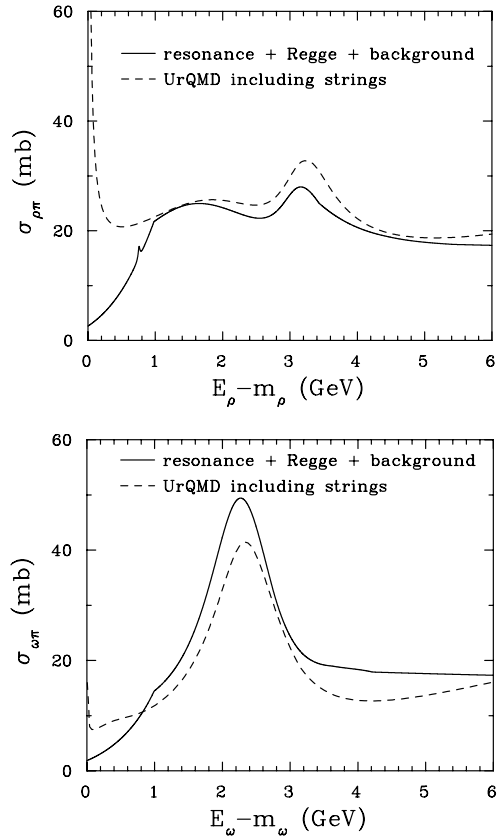


FIG. 4. Cross sections for vector mesons scattering from pions: comparison of the present results with those of the UrQMD model.

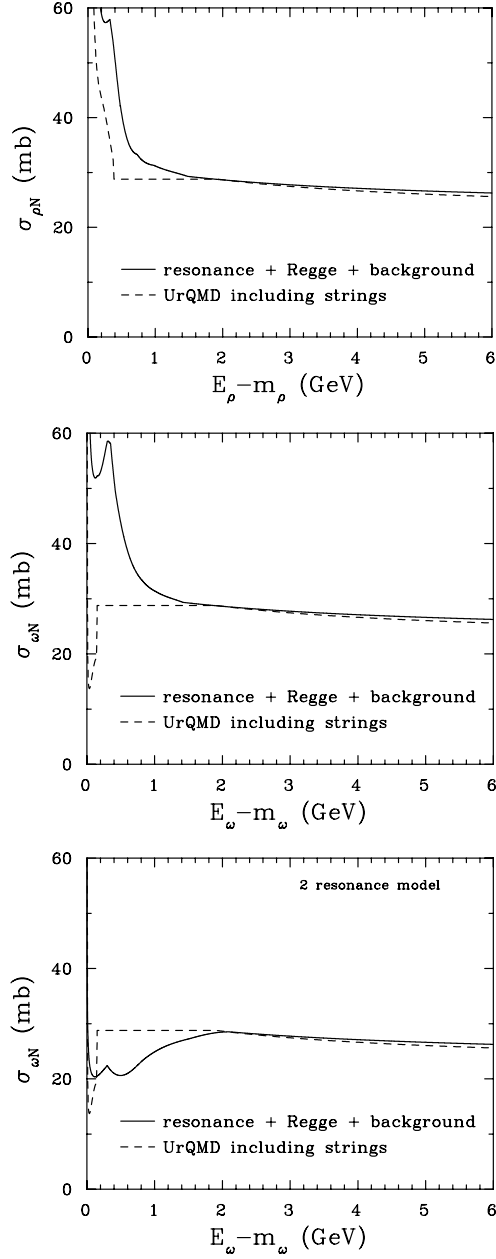


FIG. 5. Cross sections for vector mesons scattering from nucleons: comparison of the present results with those of the UrQMD model.

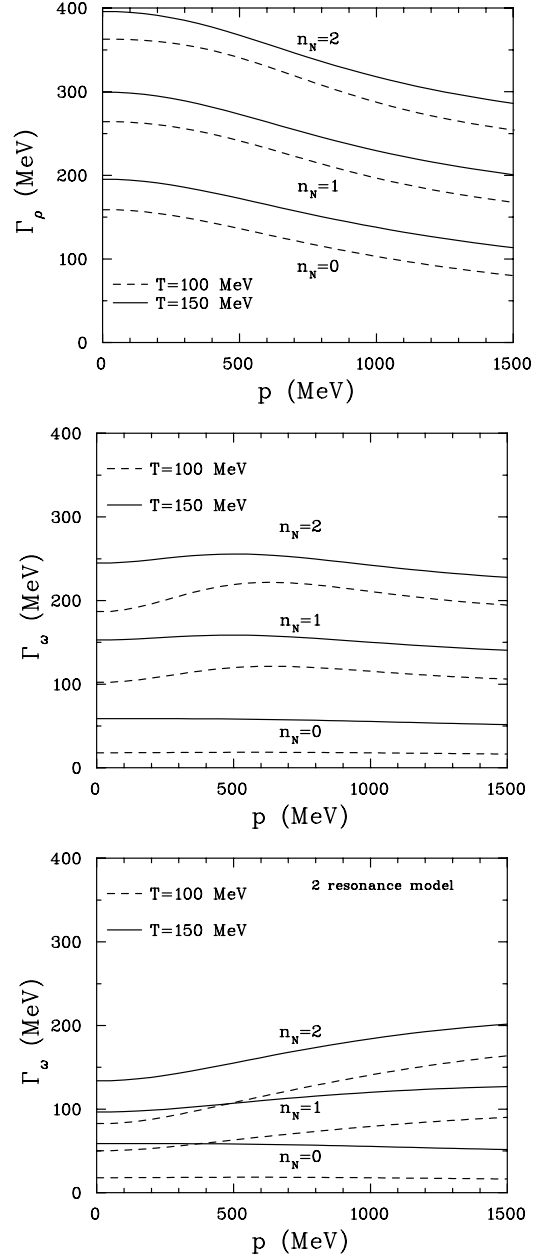


FIG. 6. The vector meson widths as a function of momentum p . Results are shown for nucleon densities of 0, n_0 and $2n_0$ (where equilibrium nuclear matter density $n_0 = 0.16 \text{ fm}^{-3}$) and temperatures of 100 and 150 MeV. For the ω meson results are given for the multi-resonance and the two-resonance models.

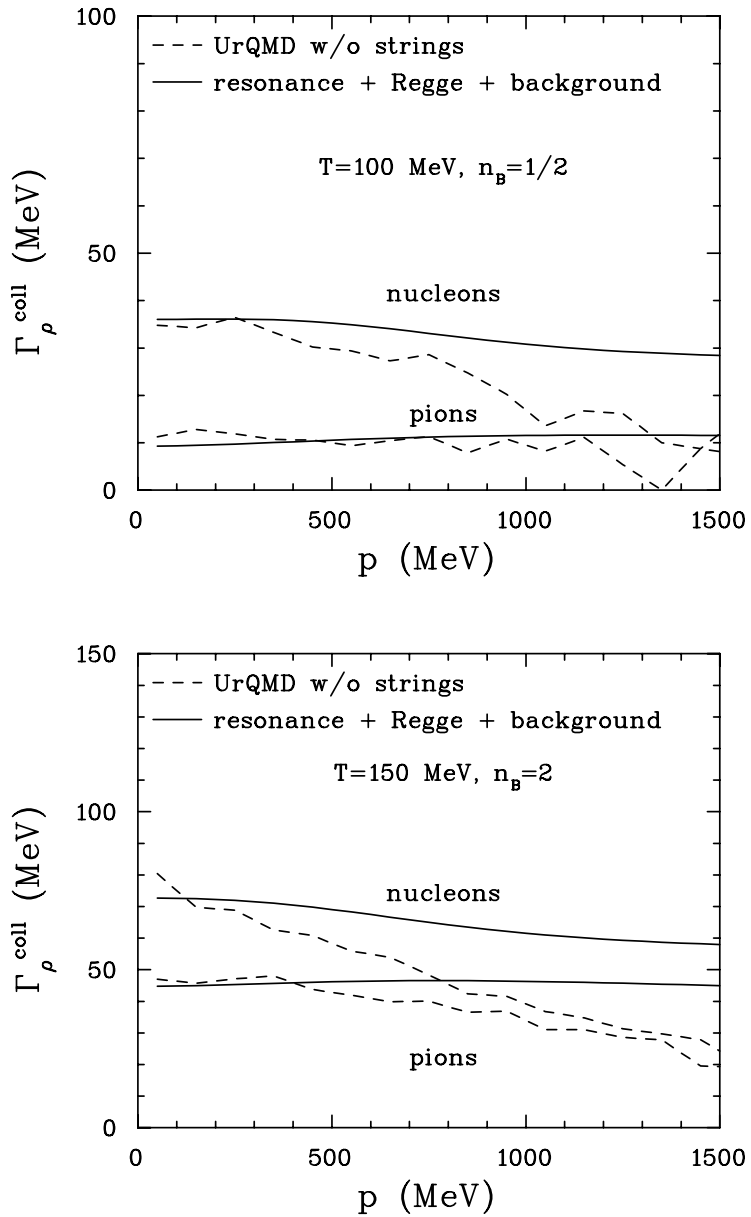


FIG. 7. Comparison of the present results with those of the UrQMD model (without strings) for the widths generated by collisions with pions or nucleons. The temperatures and baryon densities for the two cases are indicated.

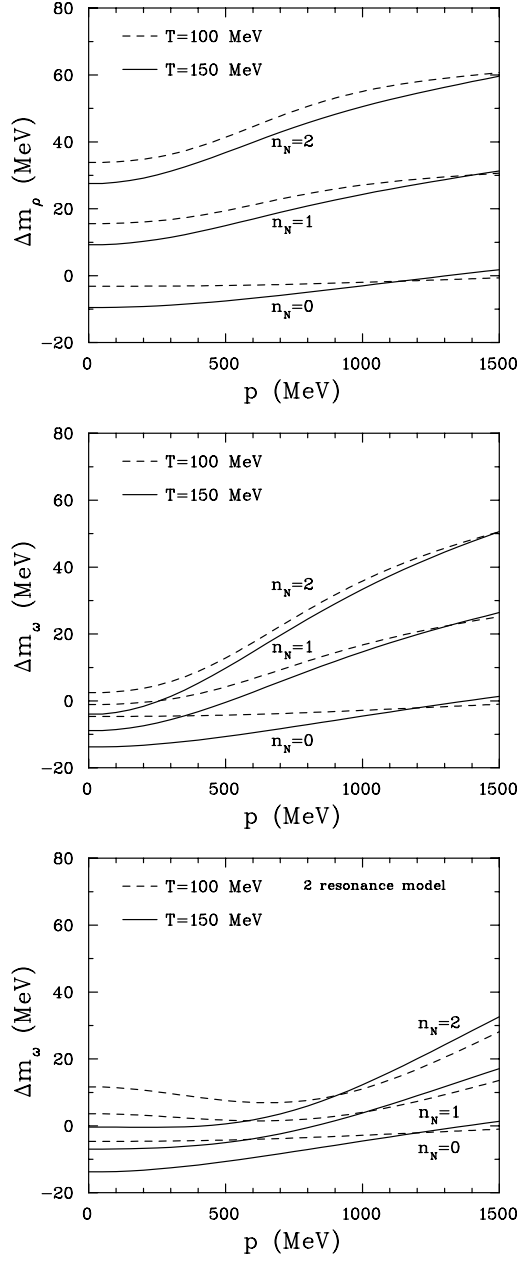


FIG. 8. As for Fig. 6, but the vector meson mass shifts.

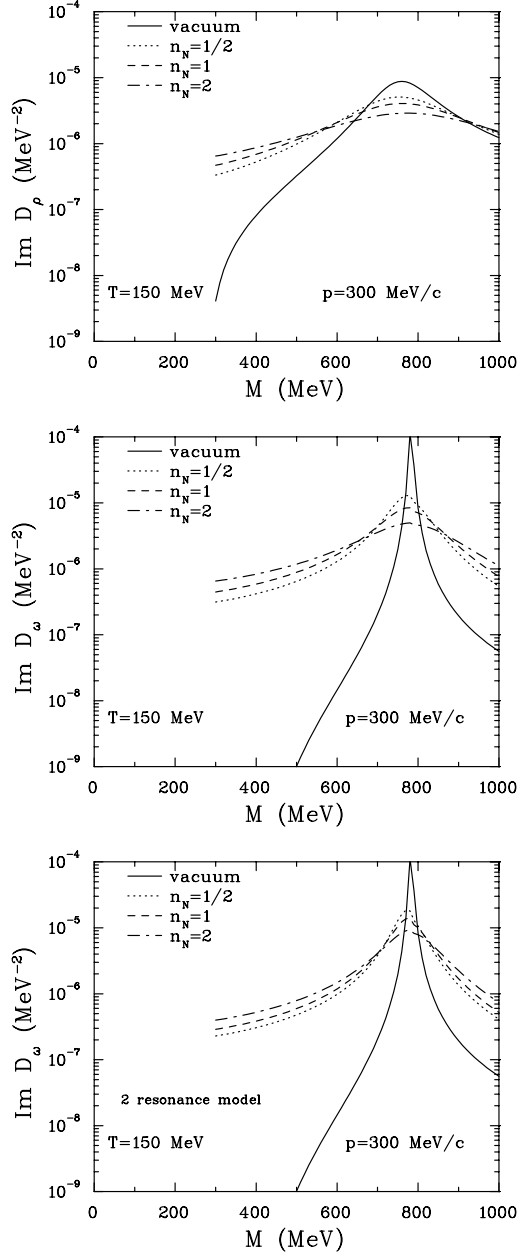


FIG. 9. The imaginary part of the vector meson propagators as a function of invariant mass for a momentum of 300 MeV/c and a temperature of 150 MeV. Results are shown for the vacuum and nucleon densities of $\frac{1}{2}n_0$, n_0 and $2n_0$. For the ω meson results are given for the multi-resonance and the two-resonance models.